

Non-ergodic metallic and insulating phases of Josephson junction chains

M. Pino^a, B.L. Altshuler^b and L.B. Ioffe^{a,c}

^a Department of Physics and Astronomy, Rutgers The State University of New Jersey,
136 Frelinghuysen rd, Piscataway, 08854 New Jersey, USA

^b Physics Department, Columbia University, New York 10027, USA

^c LPTHE, CNRS UMR 7589, Boite 126, 4 Jussieu, 75252 Paris Cedex 05, France

Abstract

Strictly speaking the laws of the conventional Statistical Physics, based on the Equipartition Postulate[1] and Ergodicity Hypothesis[2], apply only in the presence of a heat bath. Until recently this restriction was not important for real physical systems: a weak coupling with the bath was believed to be sufficient. However, the progress in both quantum gases and solid state coherent quantum devices demonstrates that the coupling to the bath can be reduced dramatically. To describe such systems properly one should revisit the very foundations of the Statistical Mechanics. We examine this general problem for the case of the Josephson junction chain and show that it displays a novel high temperature non-ergodic phase with finite resistance. With further increase of the temperature the system undergoes a transition to the fully localized state characterized by infinite resistance and exponentially long relaxation.

The remarkable feature of the closed quantum systems is the appearance of Many-Body Localization (MBL)[3]: under certain conditions the states of a many-body system are localized in the Hilbert space resembling the celebrated Anderson Localization [4] of single particle states in a random potential. MBL implies that macroscopic states of an isolated system depend on the initial conditions i.e. the time averaging does not result in equipartition distribution and

the entropy never reaches its thermodynamic value. Variation of macroscopic parameters, e.g. temperature, can delocalize the many body state. However, the delocalization does not imply the recovery of the equipartition. Such a non-ergodic behavior in isolated physical systems is the subject of this Letter.

We argue that regular Josephson junction arrays (JJA) under the conditions that are feasible to implement and control experimentally demonstrate both MBL and non-ergodic behavior. A great advantage of the Josephson circuits is the possibility to disentangle them from the environment as was demonstrated by the quantum information devices.[5] At low temperatures the conductivity σ of JJA is finite (below we call such behavior metallic), while as $T \rightarrow 0$ JJA becomes either a superconductor ($\sigma \rightarrow \infty$) or an insulator ($\sigma \rightarrow 0$)[6, 7]. We predict that at a critical temperature $T = T_c$ JJA undergoes a true phase transition into a MBL insulator ($\sigma = 0$ for $T > T_c$). Remarkably already in the metallic state JJA becomes nonergodic and can not be properly described by the conventional Statistical Mechanics.

JJA is characterized by the set of phases $\{\phi_i\}$ and charges $\{q_i\}$ of the superconducting islands, ϕ_i and q_i for each i are canonically conjugated. The Hamiltonian H is the combination of the charging energies of the islands with the Josephson coupling energies. Assuming that the ground capacitance of the islands dominates their mutual capacitances (this assump-

tion is not crucial for the qualitative conclusions) we can write H as

$$H = \sum_i \left[\frac{1}{2} E_C q_i^2 + E_J (1 - \cos \phi_i) \right] \quad (1)$$

The ground state of the model (1) is determined by the ratio of the Josephson and charging energies, E_J/E_C that controls the strength of quantum fluctuations: JJA is an insulator at $E_J/E_C < \eta$ and a superconductor at $E_J/E_C > \eta$ [6, 7] with $\eta \approx 0.63$ (see Supplemental materials). The quantum transition at $E_J/E_C = \eta$ belongs to the Berezinsky-Kosterlitz-Thouless universality class [8]. Away from the ground state in addition to E_J/E_C there appears dimensionless parameter U/E_J where U is the energy per superconducting island ($U = T$ in the thermodynamic equilibrium at $T \ll E_J$).

The main qualitative finding of this paper is the appearance of a non-ergodic and highly resistive “bad metal” phase at high temperatures, $T/E_J > 1$, which at $T \geq T_c \approx E_J^2/E_C$ undergoes the transition to the MBL insulator. In contrast to the $T = 0$ behavior, these results are robust, e.g. are insensitive to the presence of static random charges. The full phase diagram in the variables E_J/E_C , T/E_J is shown in Fig. 1. We confirmed numerically that the bad metal persists in the classical limit although $T_c \rightarrow \infty$; it is characterized by the exponential growth of the resistance with T and violation of thermodynamic identities. We support these findings by semi-quantitative theoretical arguments. Finally, we present the results of numerical diagonalization and tDMRG (time Density Matrix Renormalization Group[9]) of *quantum* systems that demonstrate both the non-ergodic bad metal and the MBL insulator.

It is natural to compare the non-ergodic state of JJA with a conventional glass characterized by infinitely many metastable states. The glass entropy does not vanish at $T = 0$, i. e. when heated from $T = 0$ to the melting temperature the glass releases less entropy than the crystal (Kauzmann paradox [10]). Similarly to glasses JJA demonstrates non-ergodic behavior in both quantum and classical regimes. However the ergodicity violation emerges as high rather than low temperatures transforming

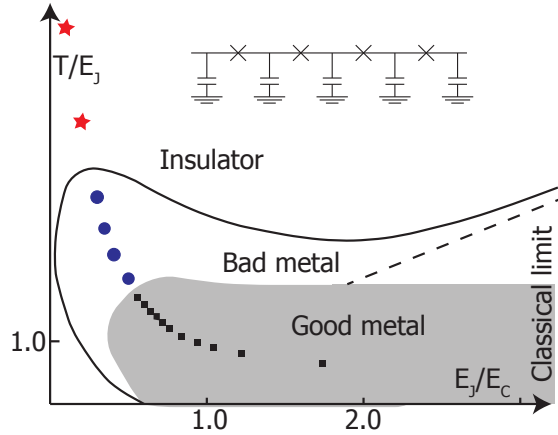


Fig. 1: Phase diagram of one dimensional Josephson junction array. The MBL phase transition separates the non-ergodic bad metal with exponentially large but finite resistance from the insulator with infinite resistance. Cooling the non-ergodic bad metal transforms it into a good ergodic metal. The points show approximate positions of the effective T/E_J for the quantum problem with a finite number of charging states. The red stars indicate insulator, blue circles bad metal, and squares good metal.

Kauzmann paradox into an apparent temperature divergence (see below).

Qualitative arguments for MBL transition. In a highly excited state $U \gg E_J$ the charging energy dominates: $E_C q^2 \sim U \gg E_J$. Accordingly, the value of the charge, $|q_i|$, and charge difference on neighboring sites, $\delta q_i = |q_i - q_{i+1}|$ are of the order of $q \sim \delta q \sim \sqrt{U/E_C}$. The energy cost of a unit charge transfer between two sites $\delta E \sim \sqrt{U E_C}$ exceeds the matrix element of the charge transfer, $E_J/2$, as long as $U \gg U_{MBL} = E_J^2/E_C$. According to [4, 3] the system is a non-ergodic MBL insulator under this condition. Thus, we expect the transition to MBL phase at $T_c/E_J \propto E_J/E_C$ with the numerical prefactor close to unity (see supplemental materials).

If $E_J/E_C \gg 1$ and $U \sim T \ll E_J$ the conductivity limited by thermally activated phase slips is exponentially large, $\sigma \sim \exp(E_J/T)$ [11, 12]. As we show be-

low, at $T \gg E_J$ in the metallic phase conductivity is exponentially small, $\sigma \sim \exp(-T/E_J)$, even far from the transition, $E_J \ll T \ll E_J^2/E_C$. The resistance in this state can exceed $R_Q = h/(2e)^2$ dramatically and still display the “metallic” temperature behavior ($dR/dT > 0$).

Classical regime is realized at $E_C \rightarrow 0$ for fixed E_J and T . One can express the charge of an island q through the dimensionless time $\tau = \sqrt{E_J E_C} t$ as $q = \sqrt{E_J/E_C} d\phi/d\tau$. Since $q \sim \sqrt{E_J/E_C} \gg 1$, one can neglect the charge quantization and use the equations of motion

$$\frac{d^2 \phi_i}{d\tau^2} = \sin(\phi_{i+1} - \phi_i) + \sin(\phi_{i-1} - \phi_i), \quad (2)$$

Here $i = 1, \dots, L$ and the boundary conditions are $\phi_0 = \phi_{L+1} = 0$. We solve these equations for the various initial conditions corresponding to a given total energy and compute the energy U_S contained in a part of the whole chain of the length $1 \ll l \ll L$ as a function of τ .

The ergodicity implies familiar thermodynamic identities. e.g.

$$\left(\langle U_S^2 \rangle - \langle U_S \rangle^2 \right) / T^2 = d \langle U_S \rangle / dT \quad (3)$$

This relation between the average energy of the subsystem, $\langle U_S \rangle$ and its second moment $\langle U_S^2 \rangle$ turns out to be invalid for a bad metal. To demonstrate this we evaluated the average energy per site in this subsystem, $u = \overline{\langle U_S \rangle}_\tau / (E_J l)$ and the temporal fluctuations of this energy, $w_\tau = \left(\langle U_S^2 \rangle_\tau - \langle U_S \rangle_\tau^2 \right) / (E_J^2 l)$. Here $\langle \dots \rangle_\tau$ and the bar denote correspondingly averaging over the time¹ and over the ensemble of the initial conditions.

From (1) it follows that $u = T/(2E_J)$ at $T \gg E_J$ ($u(T)$ -function is evaluated for arbitrary T/E_J in supplemental materials). One can thus rewrite (3) as

$$w = \frac{T^2}{E_J} \frac{du}{dT} \approx 2u^2 \quad (4)$$

Results of the numerical solution of (2) are compared with (3) in Fig. 2. For any given evolution

¹ Given the evolution time τ_{av} $\langle \dots \rangle_\tau$ averaging means averaging over the time interval τ_{ev} after initial evolution for time τ_{ev} .

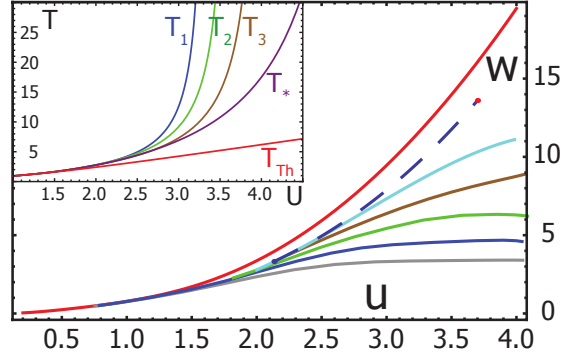


Fig. 2: Energy fluctuations as a function of average energy per island for different evolution times ($\tau_{ev} = 1, 2, 4, 8, 16 \times 10^4$) in a small system; the dashed line is the extrapolation to infinite times as explained in the text. A single point (red) obtained by direct computations up to $\tau_{ev} = 2 \times 10^6$ at which time scales the time dependence practically disappears for $L \lesssim 100$. The upper (red) curve corresponds to the thermodynamic identity (3). The insert shows the effective temperature defined by the energy fluctuations determined at different time scales: $\tau_{ev} = 2, 4, 8 \times 10^4$ ($T_1 - T_3$ respectively) and by their extrapolation to infinite times (T_*), their comparison with the temperature expected in thermodynamic equilibrium, T_{Th} .

time, τ_{ev} , the computed $w_\tau(u)$ -dependence saturates instead of increasing as u^2 (4). At a fixed u , $w_\tau(u)$ increases with time extremely slowly. Below we argue that $w_\tau(u)$ does not reach its thermodynamic value even at $\tau \rightarrow \infty$. Violation of the thermodynamic identity implies that temperature is ill defined, so the average energy u rather than T is the proper control parameter. The effective temperature defined as $T_*(u) = E_J / \int_0^u du/w(u)$, is shown in the insert to Fig. 2.

Qualitative interpretation. Large dispersion of charges on adjacent islands, $i, i+1$ at $u \gg 1$ implies quick change of the phase differences, $\phi_i - \phi_{i+1}$, with time. Typical current between the two neighbors $E_J \sin(\phi_i - \phi_{i+1})$ time-averages almost to zero.

However, accidentally the frequencies, $\omega_i = d\phi_i/dt$, get close. In the classical limit the difference $\omega_i - \omega_{i+1}$ can be arbitrary small. Such pair of islands is characterized by one periodic in time phase difference. Contrarily, three consecutive islands with close frequencies $|\omega_i - \omega_{i+1}| \sim |\omega_i - \omega_{i-1}| \lesssim 1$ experience chaotic dynamics that contains arbitrary small frequencies, similarly to work [13]. For uncorrelated frequencies with variances $u \gg 1$, a triad of islands ($i-1, i, i+1$) is chaotic with the probability $1/u \ll 1$, i.e. such triads are separated by large quiet regions of a typical size $r_t \sim u \gg 1$. The low frequency noise generated by a chaotic triad decreases exponentially deep inside a quiet region. Provided that $\omega \ll \omega_{i+m}$, $m = 0 \dots r$ the superconducting order parameter $z_i(\omega) = \int d\tau \exp(i\phi_i + i\omega\tau)$ at site i satisfies the recursion relation

$$z_{i+r}(\omega) = z_i(\omega) \prod_{m=0}^{r-1} \frac{1}{2\omega_{i+m}^2} \quad (5)$$

which implies the log-normal distribution for the resistances $R_{j,j+r}$ of quiet regions (see Supplemental materials):

$$\langle \ln^2(R/R_t) \rangle = \ln R_t \quad (6)$$

$$\ln R_t = \langle \ln R \rangle = u \ln(u) \quad (7)$$

where R_t is the typical resistance of a quiet region. The resistance of the whole array is the sum of the resistances of the quiet regions. The mean number of these regions in the chain equals to $N = L/r_t \gg 1$, its fluctuations being negligible. For the log normal distribution the average resistance of a quiet region, $\langle R \rangle$, is given by $\langle R \rangle = R_t^{3/2}$. For the resistivity, ρ , we thus have $\rho = N \langle R \rangle / L = R_t^{3/2}/r_t$. According to (7)

$$\ln \rho r_t \approx \frac{3}{2} (\gamma + \ln u) r_t \approx u(\ln u + \gamma) \quad (8)$$

where $\gamma = 0.577$ is Euler constant.

In order to determine the current caused by voltage V across the chain we solved the equations (2) with modified boundary conditions, $\phi_0 = 0$, $\phi_{L+1} = Vt$. The results confirm the prediction (8), see Fig. 3. The range of the resistances set by realistic computation time is too small to detect the logarithmic factor in (8,7), however, a relatively large slope,

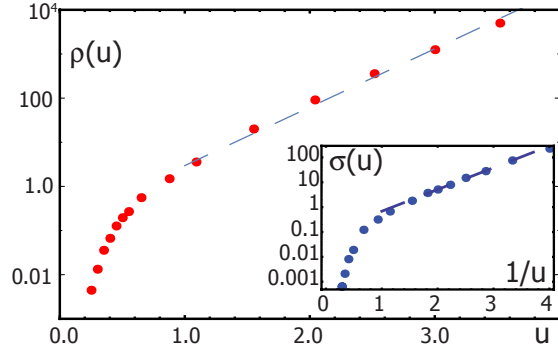


Fig. 3: Resistivity as a function of the internal energy. At high energies resistivity is exponentially large due to large regions of almost frozen charges (see text). Insert: at low energies (temperatures) exponentially large conductivity is limited by exponentially rare phase slips. High u points require computation times $\tau_{ev} \sim 10^8$.

$d \ln \rho / du \approx 3.0$ at $u = 3.5$ is consistent with (8) that gives $d \ln \rho / du \approx 2.5 + 1.5 \ln u - 1/u$.

The qualitative picture of triads separated by log-normally distributed resistances of silent regions allows one to understand the long time relaxation of $w_\tau(u)$ in the subsystem of length l (see Fig. 2). Each resistance can be viewed as a barrier with a tunneling rate $\sim 1/R$. For a given time τ the barriers with $\tau \ll R$ can be considered impenetrable, whilst the barriers with $\tau \gg R$ can be neglected. As a result, the barriers with $R \geq \tau$ break the system into essentially independent quasiequilibrium regions (QER) of the typical size

$$l_\tau \sim \frac{r_t}{\sqrt{2\pi \ln R_t}} \exp \left[\frac{\ln^2(\tau/R_t)}{2 \ln R_t} \right]. \quad (9)$$

If $l \gg r_t$ and $\tau \lesssim \exp \left[\sqrt{\ln(l/r_t) \ln R_t} \right]$ the subsystem contains $l_\tau/l \gg 1$ QER, so that $w \propto l_\tau/l$. At longer times, $l_\tau \gg l$, the subsystem is in equilibrium with a particular QER and $w \propto l/l_\tau$. The full dependence on time can be interpolated as

$$w_\tau = \frac{w_\infty}{1 + \beta \exp(-\alpha \ln^2(\tau/\tau_0))} \quad (10)$$

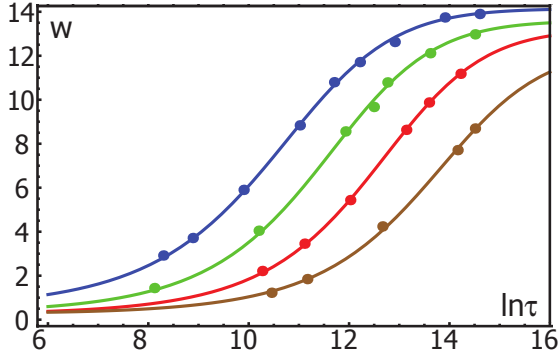


Fig. 4: Time dependence of energy fluctuations for the subsystems of different sizes $l = 10, 20, 40, 80$ (left to right) and their fits to log-normal law (10). The length of the full system was $L = 5l$. The best fit shown here corresponds to the value $\alpha = 0.05$, $\beta/l = 1.0 - 1.5$ and $\ln \tau_0 \approx 3.0 - 4.5$. The values for larger sizes ($\beta/l \approx 1.0$ and $\ln \tau_0 \approx 4.5$) agree very well with the ones expected for R_t obtained in the computation of the resistance at $u = 3.5$: $\ln R_t \approx 5.0$. This yields $r_t \approx 5.0$, $\beta/l \approx 1.1$ and $\ln \tau_0 \approx 5.0$.

where $\alpha = (2 \ln R_t)^{-1}$, $\beta = \sqrt{\pi/\alpha}(l/r_t)$ and $\tau_0 = R_t$.

The numerical simulations confirm that the energy variance w relaxes in agreement with (10) as shown in Fig. 4. The best fit to the equation (10) yields parameters close to the expected, $\ln R_t = \ln \rho(u)r_t$, $r_t \approx u$. Extrapolation gives $w_\infty(\infty) \approx 10.0$ of $w_\infty(l)$ to large l , which is significantly smaller than thermodynamic value $w_{Th} = 14.0$ at $u = 3.5$.

Another test of the ergodicity follows from the fluctuation-dissipation theorem (FDT) that relates conductivity and current fluctuations. In the low frequency limit the noise power spectrum is $S(\omega \rightarrow 0) = 2T_{eff}/R$ where T_{eff} is the effective temperature (see Fig. 5), which we extracted from the numerical data. We found that $T_{eff} > T_{Th}$ for $u \gtrsim 1$, where T_{Th} is thermodynamic temperature. In particular, $T_{eff} \approx 1.6T_{Th}$ for $u = 3.5$, which is close to $T_*(u)$ shown on the inset to Fig. 2.

Quantum behavior. In contrast to a classical limit $E_C \rightarrow 0$ in the quantum regime $E_C > 0$ we ex-

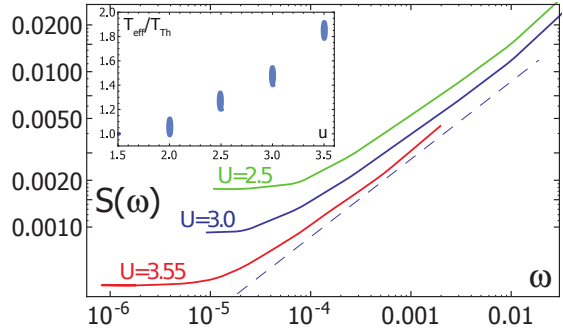


Fig. 5: Spectrum of current noise fluctuations, $S(\omega)$ for different internal energies, $U = 2.5, 3.0, 3.55$. The dashed line shows $S(\omega) \sim \omega^{1/2}$ dependence. Insert shows the effective temperature determined from FDT relation.

pect at $T = T_c$ a MBL phase transition between two non-ergodic states: the insulator ($\rho = \infty$) and a bad metal ($\rho < \infty$). For $E_J \gg E_C$ the bad metal can be described classically at $T \ll T_c \sim E_J^2/E_C$. Our previous discussion suggests that the bad metal is non-ergodic in a broad range of the parameters, T/E_J and E_J/E_C . To verify this conjecture numerically we reduced the Hilbert space of the model (1) to a finite number of charging states at each site, $q_i = 0, \pm 1, \pm 2$ (RHS model). We analyzed the time evolution of entanglement entropy, $S\{\Psi\}$ of the left half of the system. The entropy was averaged over the initial states from the ensemble of product states in the charge basis, $S_t(L) \equiv \langle S\{\Psi\} \rangle_{\Psi_{in}}$ that correspond to zero total charge. As a result, we obtained the Gibbs entropy at $T = \infty$ (all states have the same weight $\exp(-H/T) \equiv 1$)

The insert to Fig. 6 shows the time dependence of the entropy at $E_J/E_C = 0.3$ which corresponds to the bad metal regime (see below). A slow saturation of the entropy follows its quick initial increase. It is crucial that the saturation constant, $S_\infty(L)$ is significantly less than its maximal value, $S_{Th}(L) = L \ln 5$ expected at $T = \infty$ equilibrium. Furthermore, $dS_\infty(L)/dL < \ln 5$, indicating that $S_\infty - S_{Th}$ is extensive and the system is essentially non-ergodic.

Fig. 6 presents S_∞ as a function of E_J/E_C . Note that S_∞ is measurably less than S_{Th} for $E_J/E_C <$

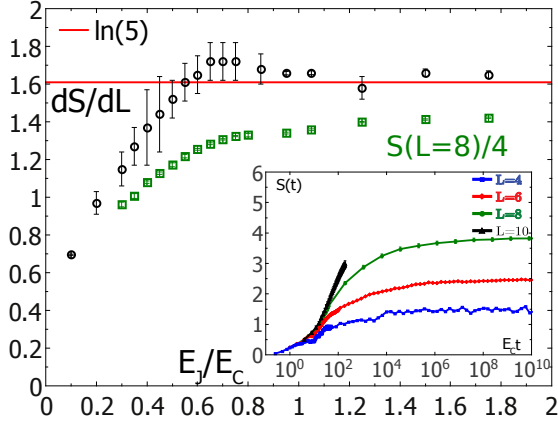


Fig. 6: Entropy per spin in thermodynamic limit extrapolated to $t = \infty$. The insert shows $S(t)$ dependence in the bad metal regime at $E_J/E_C = 0.3$ that shows slow relaxation of the entropy to its saturation value.

0.6 – 1. For $E_J/E_C \gg 1$, the entropy saturation is quick and the accuracy of the simulations does not allow us to distinguish S_∞ from S_{Th} (see Supplementing material). We thus are unable to conclude if the system is truly ergodic or weakly non-ergodic at $E_J/E_C \gg 1$. The former behavior would imply a genuine phase transition between bad and good metals, while the latter corresponds to a crossover.

Deep in the insulator the time dependence of the entropy is extremely slow, roughly linear in $\ln t$ in a wide time interval (see Supplemental materials). This resembles the results of the works [14, 15] for the conventional disordered insulators. The extremely long relaxation times can be attributed to rare pairs of almost degenerate states localized within different halves of the system. The exponential decay with distance of the tunneling amplitude that entangles them leads to the exponentially slow relaxation.

In order to locate the MBL transition we analyzed the time dependence of the charge fluctuations. In a metal the charge fluctuations relaxation rate depends weakly (as a power law) on the sample size in contrast to the exponential dependence in the insulator. Comparing the dependences of the rates on the system size for different E_J/E_C (see Fig. 7) we see that the tran-

sition happens in the interval $0.05 < E_J/E_C < 0.3$.

The variances of the charge in the RHS model at $T = \infty$ and the problem (1) at finite T coincide at $T = 2E_C$. Thus, we expect that the results of the quantum simulations describe the behavior of the model (1) at $T/E_J \sim E_C/E_J$ yielding the hyperbola shown in Fig. 1. The MBL transition at $E_J/E_C \sim 0.2$ in $T = \infty$ RHS model corresponds to the transition temperature $T_c \sim 10E_J$ in model (1). The transition line shown in Fig. 1 is a natural connection of this point with $T_c \approx E_J^2/E_C$ asymptotic at $E_J/E_C \gg 1$ discussed above. The maximum of the transition temperature is natural because the quantum fluctuations are largest at $E_J \sim E_C$.

Possible experimental realization. MBL and the violation of the ergodicity can be observed only at sufficiently low temperatures when one can neglect the effects of thermally excited quasiparticles which form the environment to model (1). This limits temperatures to $T \lesssim 0.1\Delta$ where Δ is superconducting gap. In order to explore the phase diagram one has to vary both T/E_J and E_J/E_C in the intervals $1 \lesssim T/E_J \lesssim 5$ and $0.1 \lesssim E_J/E_C \lesssim 5$. The former condition can be satisfied if each junction is implemented as a SQUID loop with individual Josephson energy $E_J^{(0)} \sim T_{max} = 0.1\Delta$ so that $E_J = 2 \cos(e\Phi/\pi\hbar)E_J$ where Φ is flux through the loop. The latter condition requires enhancing ground capacitance of each island which should exceed the capacitance of the junctions in order for the model (1) to be relevant. Realistic measurements of such array include resistance $R(T, E_J)$ and current noise. Here we predict a fast growth with temperature and divergence at T_c of the resistivity and violation of FDT.

In conclusion, we presented strong numerical evidences for the MBL transition and its semi-quantitative description in a *regular*, disorder free² Josephson chain. Probably the most exciting finding is the intermediate non-ergodic conducting phase (bad metal) between the MBL insulator and good ergodic metal. This phase distinguishes Joseph-

² When this work was finished we learnt about the numerical studies [16, 17] that reports MBL in disorder free 1D systems, in contrast the work [18] reports the absence of MBL in such systems. All these works studied models different from ours.

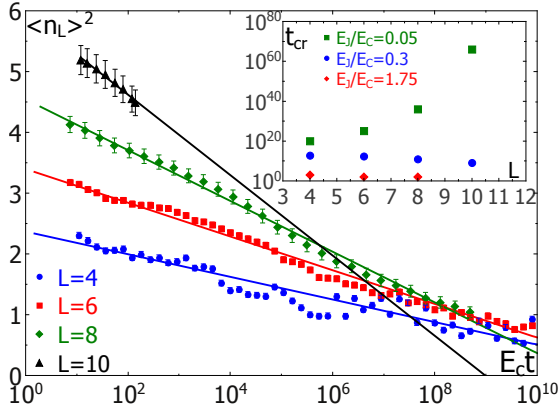


Fig. 7: Charge relaxation in a bad metal ($E_J/E_C = 0.3$). The characteristic time scale, t_{cr} , can be defined by the extrapolated crossing point of $\langle n^2 \rangle$ with t -axis. The crossing point t_{cr} shows dramatically different behavior for the insulator and metal as shown by insert: in the good metal this time is very short, in the bad metal it is dramatically longer but does not increase with size whilst in insulator it is extremely long and grows with size.

son junction chain from the spin1/2 Heisenberg one-dimensional model in the random field, [19, 20, 21], where the ergodicity is believed to be violated *only* in the MBL regime[21]. The ergodicity violation in a wide range of parameters is in contrast to the one particle Anderson localization in a finite-dimensional space where the non-ergodic behavior is limited to the critical point. However, the signatures of the “non-Gibbs regime” in the discrete nonlinear Schrodinger equation [22, 23], the appearance of the non-ergodic states in a single particle problem on the Bethe lattice as well as the dominance of single path relaxation close to the critical point of superconductor-insulator transitions on Bethe lattice[24, 25] make us believe that the intermediate non-ergodic phase is a generic property of MBL transition rather than an exception. Further work is needed to establish the domain of the applicability of these results as well as the nature of the transition between bad and good metals.

Methods

Simulation of the JJA in the classical regime. At large u averaging out temporal fluctuations requires exponentially long times. Moreover, at $u \gg 1$ the resistance increases with u factorially leading to a strong heating in the computation of resistance unless the measurement current is factorially small. Observation of a small current against the background of a low frequency noise requires increasingly long times. Accordingly, for the realistic evolution times $\tau_{ev} \lesssim 10^8$ the resistance can be computed only for $u < 4.0$.

Simulation of the quantum problem. The time dependence of the entropy and the charge fluctuations for system of sizes $L = 4, 6, 8$ was computed using exact diagonalization in a symmetric subspace under charge conjugation. The tDMRG method was employed for larger sizes which accuracy limits the range of times that we could study. In all simulations we impose the particle number conservation and open boundary conditions.

References

- [1] J.W. Gibbs. *Elementary Principles in Statistical Mechanics, developed with especial reference to the rational foundation of thermodynamics*. Charles Scribners Sons, New York, 1902.
- [2] L. Boltzmann. *Lectures on gas theory*, volume Part 2, Chapter 3. Berkley, 1964.
- [3] D.M. Basko, I.L. Aleiner, and B.L. Altshuler. Metal-insulator transition in a weakly interacting many-electron system with localized single-particle states. *Annals of Physics*, 321(5):1126 – 205, 2006.
- [4] P. W. Anderson. Absence of diffusion in certain random lattices. *Phys. Rev.*, 109:1492–1505, Mar 1958.
- [5] M. H. Devoret and R. J. Schoelkopf. Superconducting circuits for quantum information: An outlook. *Science*, 339(6124):1169–1174, 2013.
- [6] K.B. Efetov. Phase transitions in granulated superconductors. *Zhurnal Eksperimental’noi i Teoreticheskoi Fiziki*, 78(5):2017 – 32, 1980.

-
- [7] R. Fazio and H. van der Zant. Quantum phase transitions and vortex dynamics in superconducting networks. *Physics Reports*, 355(4):235 – 334, 2001.
- [8] J.M. Kosterlitz and D.J. Thouless. *40 Years of Berenzinskii-Kosterlitz-Thouless Theory*, chapter Early work on defect driven phase transitions, pages 1 – 67. World Scientific Publishing, Singapore, 2013.
- [9] Steven R. White. Density matrix formulation for quantum renormalization groups. *Phys. Rev. Lett.*, 69:2863–2866, Nov 1992.
- [10] Walter Kauzmann. The nature of the glassy state and the behavior of liquids at low temperatures. *Chem. Rev.*, 42:219–256, 1948.
- [11] M. Tinkham. *Introduction to superconductivity*. McGraw-Hill, 1996.
- [12] V.V. Schmidt. *The Physics of Superconductors: Introduction to Fundamentals and Applications*. Springer, Berlin, 2002.
- [13] B.V. Chirikov. A universal instability of many-dimensional oscillator systems. *Physics Reports*, 52(5):265 – 379, 1979.
- [14] Jens H. Bardarson, Frank Pollmann, and Joel E. Moore. Unbounded growth of entanglement in models of many-body localization. *Phys. Rev. Lett.*, 109:017202, 2012.
- [15] Maksym Serbyn, Z. Papić, and Dmitry A. Abanin. Universal slow growth of entanglement in interacting strongly disordered systems. *Phys. Rev. Lett.*, 110:260601, 2013.
- [16] N. Y. Yao, C. R. Laumann, J. I. Cirac, M.D. Lukin, and J.E. Moore. Quasi many-body localization in translation invariant systems, 2014.
- [17] Mauro Schiulaz, Alessandro Silva, and Markus Müller. Dynamics in many-body localized quantum systems without disorder, 2014.
- [18] Z. Papić, E. M. Stoudenmire, and Dmitry A. Abanin. Is many-body localization possible in the absence of disorder?, 2015.
- [19] V. Oganesyan and D.A. Huse. Localization of interacting fermions at high temperature. *Physical Review B*, 75(15):155111 – 1, 2007.
- [20] V. Oganesyan, A. Pal, and D.A. Huse. Energy transport in disordered classical spin chains. *Physical Review B (Condensed Matter and Materials Physics)*, 80(11):115104, 2009.
- [21] D.J. Luitz, N Lafflorencie, and F. Alet. Many-body localization edge in the random field heisenberd chain. ArXiv: 1411.0660 (2014).
- [22] K.O. Rasmussen, T. Cretegny, P.G. Kevrekidis, and N. Gronbech-Jensen. Statistical mechanics of a discrete nonlinear system. *Physical Review Letters*, 84(17):3740, 2000.
- [23] S. Flach and A.V. Gorbach. Discrete breathers - advances in theory and applications. *Physics Reports*, 467(1-3):1, 2008.
- [24] M.V. Feigel'man, L.B. Ioffe, and M. Mezard. Superconductor-insulator transition and energy localization. *Physical Review B*, 82(18):184534, 2010.
- [25] E. Cuevas, M. Feigel'man, L. Ioffe, and M. Mezard. Level statistics of disordered spin-1/2 systems and materials with localized cooper pairs. *Nature Communications*, 3:1128, 2012.
- [26] P. Buonsante and A. Vezzani. Ground-state fidelity and bipartite entanglement in the bose-hubbard model. *Phys. Rev. Lett.*, 98:110601, Mar 2007.
- [27] M. Pino, J. Prior, A. M. Somoza, D. Jaksch, and S. R. Clark. Reentrance and entanglement in the one-dimensional bose-hubbard model. *Phys. Rev. A*, 86:023631, Aug 2012.

Acknowledgment

We are grateful to I.L. Aleiner, M. Feigelman, S. Flach, V.E. Kravtsov and A.M. Polyakov for useful discussions. The work was supported in part by

grants from the Templeton Foundation (40381), ARO (W911NF-13-1-0431) and ANR QuDec.

Supplemental materials

1 Free energy of the chain in thermodynamic equilibrium

Evaluation of the free energy with Hamiltonian (1) gives

$$F = \frac{1}{2}T \ln \left(\frac{E_C}{2\pi T} \right) - T \ln [I_0(E_J/T)]$$

which allows us to express u in terms of T :

$$u = \frac{T}{2E_J} + \left(1 - \frac{I_1(E_J/T)}{I_0(E_J/T)} \right) \quad (11)$$

Here $I_\alpha(x)$ are modified Bessel functions. Using (11) one can check the validity of (3), which takes the form $w = T^2 du/dT$.

2 Noise distribution.

At high temperatures the frequencies of individual phases are typically large, $\omega_i \gg 1$ which allows to solve the equations (2) in perturbation theory. Furthermore, because the effect of noise decreases exponentially with distance one can use the forward propagation approximation in which the evolution of the next phase is determined exclusively by the previous one

$$\frac{d^2 \phi_i}{d\tau^2} = -\sin(\phi_i - \phi_{i-1}) \quad (12)$$

Looking for the solution in the form $\phi_i = \omega_i \tau + \delta\phi_i(\tau)$ and introducing the notation

$$e^{i\phi_i} = \int d\omega e^{-i\omega\tau} z_i(\omega)$$

for the noise at site i we get

$$\delta\phi_i = \frac{1}{(\omega_i - \omega)^2} \text{Im} z_{i-1}(\omega) e^{i(\omega - \omega_i)\tau} \quad (13)$$

We are interested in the propagation of the low frequency harmonics of the noise, $\omega \ll \omega_i$. Neglecting the high frequency components of the noise one obtains from (13) the noise recursion

$$z_i(\omega) = \frac{1}{2(\omega_i - \omega)^2} z_{i-1}(\omega) \quad (14)$$

Iterations of (14) in the limit $\omega \ll \omega_i$ lead to the equation (5) of the main text. The exponential decrease of the noise away from its source in the classical regime is in agreement with the numerical computation in the quantum regime (see section 3).

The recursion (5) of the main text implies that the noise generated by a single triad at distance, $r \gg 1$ is given by a product of a large number of factors. Being a sum of a large number of random independent terms the logarithm of the noise has Gaussian distribution. Thus, at the distance $r_t \gg r \gg 1$, from the closest triad the noise distribution has a log normal form

$$P_r(\zeta) = \frac{1}{\sqrt{2\pi\zeta_*(r)}} \exp\left[-\frac{(\zeta - \zeta_*(r))^2}{2\zeta_*(r)}\right] \quad (15)$$

where $\zeta = \ln z$, $\zeta_*(r) = (\gamma + \ln u) r$, and $\gamma = 0.577$ is Euler constant. The exponential decay of the effect of a single triad (5,15) implies the charge localization. The DC charge transport in a macroscopically large array requires interaction of different triads through the quiet regions. A quiet interval $(j, j+r)$ between islands can be characterized by the resistance $R_{j,j+r} \sim z_j/z_{j+r}$. Convolution of distribution (15) with the Poisson distribution for the sizes of the quiet regions, r , yields the log-normal distribution for the resistances $R_{j,j+r}$ of quiet regions.

3 Charge propagation in quantum insulating phase.

In the insulating phase the charge transfer by distance r appears in the r^{th} order of the perturbation theory in the parameter $E_J/\sqrt{TE_c}$. For small $E_J/\sqrt{TE_c} \ll 1$ the main contribution to the amplitude, $\Psi(r)$ of this processes comes from exactly $r-1$ virtual hops between neighboring sites in the same direction (forward propagation approximation). These hops can occur in any order. Each sequence of the hops corresponds to a particular permutation, P , of $1 \dots r-1$. After $n < r-1$ hops the charging energy changes by $\Delta E_n = E_c \sum_{k \leq n} (q_{P(k)+1} - q_{P(k)})$, so that

$$\langle \ln |\Psi_{FWD}(r)| \rangle = \left\langle \ln \sum_P \frac{E_J}{2E_c |\sum_k (q_{P(k)+1} - q_{P(k)})|} \right\rangle_q$$

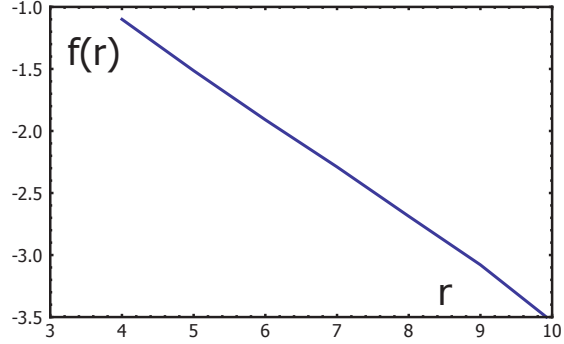


Fig. 8: Logarithm of the dimensionless amplitude of the charge transfer, $f(r)$ determined in the forward propagation approximation.

where $\langle \dots \rangle_q$ means average over charge configurations normally distributed with variance T/E_c . Rescaling the charge and factoring out the dimensionfull parameters we find that

$$\langle \ln |\Psi_{FWD}(r)| \rangle = r \ln \left(\frac{E_J}{\sqrt{TE_c}} \right) + f(r) \quad (16)$$

$$f(r) = \left\langle \ln \sum_P \frac{1}{2^{|\sum_k (q_{P(k)+1} - q_{P(k)})|}} \right\rangle_q \quad (17)$$

where average is performed over charge configurations with unit variance. The numerical evaluation of $f(r)$ shows that $f(r) \approx \eta r$ with $\eta \approx -0.3$ (see Fig. 8).

We estimate the transition temperature by demanding $\langle \ln |\Psi_{FWD}(r)| \rangle \sim \text{const}$ which gives $T_c^{FWD} \approx e^{2\eta} E_J^2/E_c$. The forward propagation approximation neglects the effects of the backscattering and level repulsion. All these apparently small effects favor the insulating behavior, thus, the actual transition is below $T_c \lesssim T_c^{FWD}$. We conclude that the numerical prefactor, $\tilde{\eta}$, in the equation for the critical temperature, $T_c = \tilde{\eta} E_J^2/E_c$ is close to one, $\tilde{\eta} \lesssim 0.5$.

The estimate of the charge transfer (16) neglects the charge discreteness which is expected to become irrelevant at $T/E_c \rightarrow \infty$. To estimate the effect of

the discreteness at finite T/E_C we note that it is dominated by the appearance of exactly zero ΔE_n for some n (resonances). Such degeneracies are lifted in the next order of the perturbation theory: the energy difference between the states with charge $q_i + 1$ and charge q_i at island i becomes

$$\begin{aligned} E(q_i + 1) - E(q_i) &= E_C(q_i + \frac{1}{2}) + \delta_i \frac{E_J^2}{E_C} \\ \delta_i &= \delta_{i,i+1} + \delta_{i-1,i} \end{aligned}$$

$$\delta_{i,i+1} = \frac{q_{i+1} - q_i - \frac{1}{2}}{\left[\frac{3}{4} - (q_{i+1} - q_i - \frac{1}{2})^2\right]^2 - (q_{i+1} - q_i - \frac{1}{2})^2}$$

Close to the transition line we estimate $\delta_i \sim (E_C/E_J)^3$, so the degeneracy is lifted by $\delta E \sim E_C^2/E_J \ll E_J$. These resonances occur with the probability E_C/E_J , at an average distance $r \sim E_J/E_C$ from each other. Close to the transition the hopping amplitude between these sites is given by

$$\Psi(r) \sim E_J \exp\left(-\frac{T - T_c}{2T_c} r\right)$$

The energy difference, ΔE , exceeds this amplitude provided that

$$\frac{T - T_c}{T_c} > \gamma' \frac{E_C}{E_J} \ln \frac{E_J}{E_C} \quad (18)$$

where $\gamma \sim 1$ is numerical coefficient. The many body localization takes place only when the condition (18) is satisfied. We conclude that the shift of the transition line upwards is small in E_C/E_J (18).

According to (17) the charge propagation is controlled by the average logarithm of the charge difference. This suggests that the simulations in which for the charge is evenly distributed in the interval $(-Q, Q)$ should resemble the simulations for the normal distribution with variance T/E_C when the two cases correspond to the same $\langle \ln q_i \rangle$ or $\langle \ln(q_i - q_{i+1}) \rangle$. Application of such criteria leads to the conclusion that restriction of the charges $-Q \leq q_i \leq Q$ at $T \rightarrow \infty$ is equivalent to the unrestricted charges (1) with effective temperature $T = \gamma' E_C Q^2$ with $\gamma' \approx 1$.

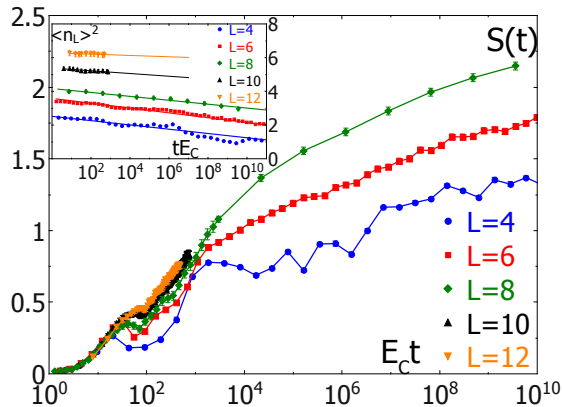


Fig. 9: Time evolution in the insulator, $E_J/E_C = 0.05$. The main panel shows slow evolution of the entropy which is roughly linear in $\ln t$ in a wide range of times. The insert shows slow relaxation of the charge which becomes even slower for longer samples.

4 Charge and entropy relaxation in quantum regime

Here we give the details of the numerical results for charge and entropy evolution in the insulating and metallic regimes that are both qualitatively different from the non-ergodic bad metal phase.

We begin with the *insulating phase*. The behavior of the entropy in a wide time range ($t < 10^{10}$) is shown in Fig. 9; one can distinguish three distinct regimes.

At shortest times ($E_C t \lesssim 20$) the entropy growth fast. The fact that this growth is identical for the systems of different sizes suggests that it is due to the particles spreading across the boundary which happens at time scales $t \sim 1/E_J$. In the intermediate time region ($20 \lesssim E_C t \lesssim 10^3$) the entropy is almost size independent for all but smallest sizes and small ($S \lesssim 1$). Similar behavior is observed for disordered systems; it is due to a small entanglement of typical excitations a bit further from the boundary or to a larger entanglement of rare excitations with exceptionally close energies. Because the amplitude of the entanglement decreases exponentially fast with dis-

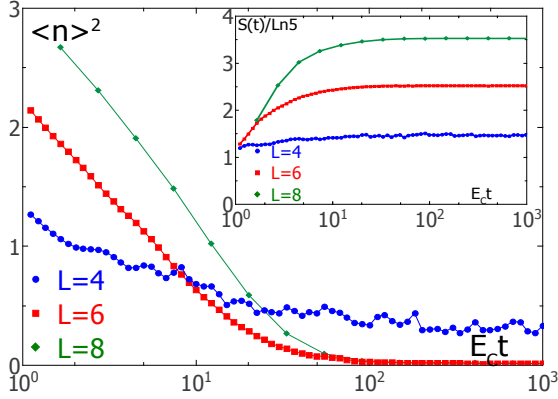


Fig. 10: Charge relaxation and entanglement entropy relaxation in a good metal realized at $E_J/E_C = 1.75$

tance the contribution to the entropy coming from the states far from the boundary is small and thus the entropy demonstrates weak size dependence in this regime.

The striking feature of the insulating state in this model is a very slow (logarithmic) growth of entropy at long times ($E_C t > 10^4$) that remains much below $\ln 5$ per site. We attribute this dynamics to degenerate charge configurations: even when located far from each other such configurations can hybridize due to a small but non zero E_J/E_C . For example, configurations connected by inversion symmetry possess a matrix element which is exponentially small in system size. The time needed to resolve this couple is thus exponentially large.

In contrast to the entropy, the charge fluctuations display simple monotonic behavior at all times. The characteristic charge relaxation time increases extremely rapidly with the system size. We conclude that this phase is a genuine insulator which phase space is separated into thermodynamically large number of independent compartments.

In a good metal there is only one regime for charge and entropy time evolution. The charge relaxes quickly and this relaxation does not show any sign of getting slower at larger system sizes, see Fig. 10. Accordingly, the entropy increases rapidly and saturates at the values that approach $L \ln 5$ for large

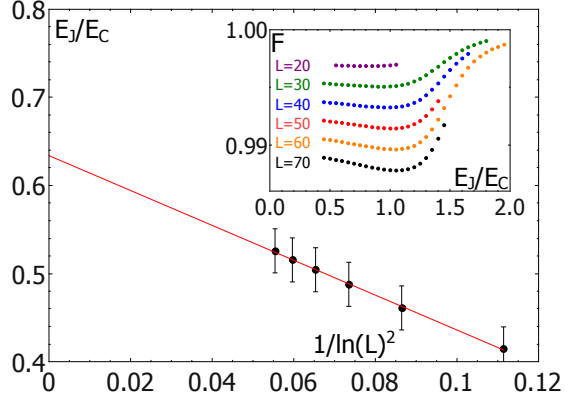


Fig. 11: The insert shows the fidelity of the ground-state as a function of E_J/E_C for different sizes L . The minimum of the fidelity as a function of $[\ln(L)]^{-2}$ appear in the main panel. The red line fits the data to a line. The location of the critical point can be extracted from the value of the fitting at origin $E_J/E_C = 0.63 \pm 0.04$.

system sizes.

5 Berezinski-Kosterlitz-Thouless critical point at zero temperature

In this section we give the details of the numerical methods that allowed us to determine the value of the ratio of Josephson to charging energies, η , for the Berezinsky-Kosterlitz-Thouless phase transition of the model (1) at zero temperature. Finite order derivatives of the energy do not display any discontinuity at this transition. Thus, we have to use more sophisticated numerical methods than the ones used in the case of second order phase transitions.

The idea of our approach is to compute the fidelity of the ground-state defined by the equation

$$F(E_J/E_C) = \langle \psi_{gs}(E_J/E_C + \delta) | \psi_{gs}(E_J/E_C) \rangle \quad (19)$$

for small δ . The result obtained by DMRG method [9] is shown in the insert of Fig. 11 as a function of E_J/E_C for different sizes. One expects that fidelity is minimal at the critical point [26]. In the main panel

of Fig. 11 we show positions of this minima as well as its extrapolation to infinite size using $E_J/E_C(L) = a[\ln(L)]^{-2} + \eta$ [27]. This procedure yields $\eta = 0.63 \pm 0.04$ cited in the main text.